Surface-plasmon distributed-feedback mid-infrared quantum cascade lasers based on hybrid plasmon/air-guided modes

A. Bousseksou, V. Moreau, R. Colombelli, C. Sirtori,
G. Patriarche, O. Mauguin, L. Largeau, G. Beaudoin and
I. Sagnes

Surface-plasmon distributed-feedback quantum cascade lasers with a first-order grating realised by the sole patterning of the top metallic contact are demonstrated. The devices have a single-mode emission with a sidemode suppression ratio greater than 20 dB. The emission wavelength at 78 K is centred at $\lambda = 7.3$ µm and has a tuning rate as a function of temperature $\simeq$0.4 nm/K.

Introduction: The quantum cascade (QC) laser is an ideal semiconductor source for the mid- and far-infrared ranges of the electromagnetic spectrum. For applications such as gas sensing and high resolution spectroscopy, single-mode operation of the devices is often required [1]. The architecture of choice to achieve single-mode emission is the use of gratings for distributed-feedback (DFB). Advances in the design and technology of QC lasers have led to the demonstration of single-mode operation at room temperature at several wavelengths [2–4]. The typical strategy to realise these single-mode lasers is to integrate a buried DFB grating within a Fabry-Perot QC laser. In this Letter we propose and demonstrate a different approach making use of surface-plasmon devices [5]. Single-mode long-wavelength surface-plasmon QC lasers have been demonstrated in the past at $\lambda \simeq 17$ µm [6]. In that case a two-metal grating was deposited, which produces a strong complex index contrast owing to the large spatial modulation of the skin depth. We show here that a pure one-metal-grating, alternating metal- and air-claddings as in Fig. 1*a*, can operate as a frequency-selecting filter and yields single-mode operation. The advantage is in the technological simplification, since there is no need for epitaxial overgrowth or semiconductor etching. Furthermore, there are ample margins for performance improvement, as we will describe in a future theoretical publication.

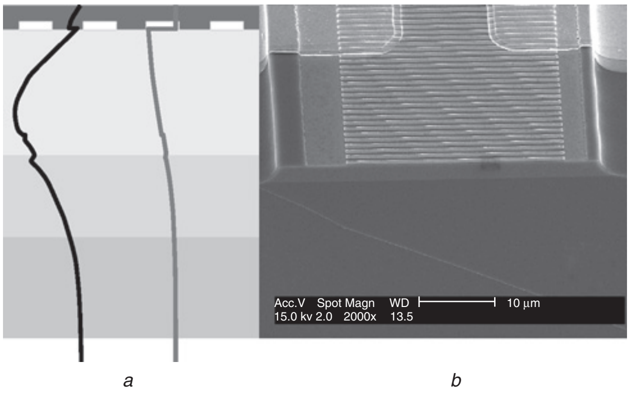

Fig. 1 *Schematics of DFB devices with distributed-feedback implemented via metal patterning only, and SEM image of edge of typical device*

a Schematics of DFB devices with distributed-feedback implemented via metal patterning only
Line sketch waveguide modes of full surface-plasmon and air-guided QC laser, respectively
b SEM image of edge of typical device
Lighter region, approximately 3 µm thick, corresponds to active-region and bottom InGaAs cladding. Metallic grating clearly visible. Its period is $\Lambda = 1.15$ µm, with 50% duty cycle

The samples were grown in a vertical-reactor, low-pressure MOVPE system (TurboDisc D180) using hydrogen as carrier gas and standard precursors (arsine (AsH3), phosphine (PH3), trimethylindium (TMI), trimethylgallium (TMGa) and trimethylaluminium (TMAl)). Our growth conditions led to an InGaAs and an InAlAs growth rate of around 1.8 ML/s for the active region. The sample contains 50 repeats of the following four-well active region + injector structure (beginning with the injection barrier, layer thicknesses in nanometres): **4.3**/1.7/**1.0**/5.3/**1.2**/5.2/**1.2**/4.4/**2.5**/3.1/**1.7**/2.9/**1.6**/2.7/**1.8**/2.6/**2.1**/2.6/**2.4**/2.4, where bold numbers refer to $Al_{0.52}In_{0.48}As$ barriers, roman type to $In_{0.53}Ga_{0.47}As$ wells, and the underlined layers are *n*-doped to 1×10^{17} cm^{-3}. The stack of active regions + injectors is sandwiched between doped thin, top InGaAs contact facilitating layers and a bottom 0.5 µm-thick InGaAs cladding layer, *n*-doped 5×10^{16} cm^{-3}.

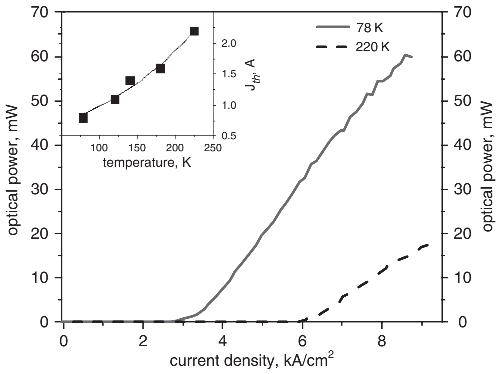

Fig. 2 *L-I-V characteristic of 750 × 45 µm device (25 µm-wide grating)*

Inset: Current threshold against heatsink temperature

Fabrication: The first processing step is the metallic-grating deposition. E-beam lithography and a lift-off process have been used to deposit 50%-duty-cycle, Ti/Au (3/200 nm-thick) gratings with different periods ($\Lambda = 1.15$, 1.17, 1.20, 1.22 and 1.25 µm). The gratings are typically 25 µm wide and a few millimetres long. Ridge waveguide resonators were then fabricated around the metallic gratings by contact optical lithography and wet etch. A SiN layer (300 nm thick) was used to provide electrical insulation. After opening of the insulating layer on top of the laser ridges through reactive ion etching, lateral Ti/Au contacts were deposited by e-beam evaporation in order to contact the grating sides. Following polishing and back contact deposition, the devices were cleaved, mounted on copper blocks, bonded and loaded into a cryostat for the measurements. Fig. 1*b* shows a scanning electron microscope image of the edge of a typical device. For this initial demonstration the ridge top widths were much larger than the grating width.

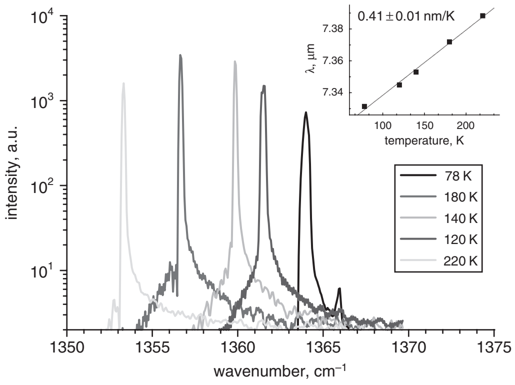

Fig. 3 *Typical laser spectra of device for different temperatures of heatsink*

Inset: Emission wavelength against heatsink temperature, showing tuning rate of $\simeq$0.4 nm/K

Characterisation: The lasers were tested in pulsed mode (50 ns pulse width, 84 kHz repetition rate). A mercury cadmium telluride (MCT) detector was used for the light-current characterisations and spectral analysis. A current-voltage characteristic at 78 K of a typical device with grating period $\Lambda = 1.15$ µm is shown in Fig. 2. The threshold voltage is $\simeq$14 V, in good agreement with the calculated design bias (14.7 V) [5]. Fig. 2 shows that the onset of lasing occurs at a current of $\simeq$0.8 A at a temperature of 78 K, corresponding to a threshold current density $J_{th} \simeq 2.6$ kA/cm^2. This is a rather high value, but it is comparable to that which is usually obtained for standard Fabry-Perot surface-plasmon QC lasers with gold plasmon-carrying layers [5]. The maximum output peak power, at 78 K, from a 750 µm-long device is $\simeq$65 mW. The power is reported without any correction due to the collection efficiency, which we estimate to be $\leq 50\%$.

The emission spectra are single-mode for a limited current range above threshold, as shown in Fig. 3. The sidemode suppression ratio is at least 20 dB, and the tuning rate is $\simeq 0.4$ nm/K (see Fig. 3, inset). This latter value is 3.5 times lower than that obtained on Fabry-Perot devices fabricated from the same material, further proving the distributed origin of the feedback in these structures. Additional modes arise at higher currents, but only one or two lateral modes appear and never is a Fabry-Perot-like spectrum recovered.

Conclusion: We have demonstrated single-mode emission from surface-plasmon QC lasers, where the distributed-feedback is achieved via the implementation of a metal grating in the sole patterning of the top metal contacts. The devices exhibit a >20 dB sidemode suppression ratio, and a tuning rate of $\simeq 0.4$ nm/K. The DFB devices have similar J_{th} as typical surface-plasmon QC lasers without grating and with Ti/Au plasmon-carrying layers, but the maximum operating temperature is lower ($T_{max} \simeq 225$ K against 265 K), possibly due to the non-optimised geometry of the devices. The performances need to be improved. Major improvements are expected from (i) process optimisation, by reducing the size difference between the grating and the ridge width, and (ii) grating duty-cycle reduction. Initial theoretical results, which will be thoroughly presented in a future publication, suggest in fact that modes with very low propagation losses can appear if the grating duty-cycle is reduced. This is not only related to the reduction of the surface covered by metal, but also to a coupling mechanism between surface-plasmon and air-guided modes (see scheme in Fig. 1*a*). This latter mechanism is reminiscent of the effect described in [7]. We believe that this technology offers the opportunity of an extremely simple implementation of single-mode DFB lasers, for applications that require device operation in pulsed mode.

Acknowledgments: We thank F. Julien, M. Carras, S. Laurent and J. Teissier for useful discussions. We gratefully acknowledge support from ANR-06-NANO-047 'MetalGuide'. Device fabrication was performed at the nano-centre CTU-IEF-Minerve which was partially funded by the 'Conseil Général de l'Essonne'. This work was conducted as part of a EURYI scheme award. See www.esf.org/euryi.

18 March 2008
Electronics Letters online no: 20080756
doi: 10.1049/el:20080756

A. Bousseksou, V. Moreau and R. Colombelli (*Institut d'Electronique Fondamentale, Université Paris Sud and CNRS, UMR8622, Orsay 91405, France*)

E-mail: colombel@ief.u-psud.fr

C. Sirtori (*Laboratoire MPQ, Université Paris7 and CNRS, UMR7162, Paris 75013, France*)

G. Patriarche, O. Mauguin, L. Largeau, G. Beaudoin and I. Sagnes (*CNRS/LPN, Laboratoire de Photonique et de Nanostructures, Route de Nozay, Marcoussis 91460, France*)

References

1 Kosterev, A., *et al.*: 'Chemical sensors based on quantum cascade lasers', *IEEE J. Quantum Electron.*, 2002, **38**, p. 582
2 Lee, B.G., *et al.*: 'Widely tunable single-mode quantum cascade laser source for mid-infrared spectroscopy', *Appl. Phys. Lett.*, 2007, **91**, p. 231101
3 Darvish, S.R., *et al.*: 'High-power, continuous-wave operation of distributed-feedback quantum-cascade lasers at $\lambda \approx 7.8$ μm', *Appl. Phys. Lett.*, 2006, **89**, p. 251119
4 Blaser, S., *et al.*: 'Room-temperature, continuous-wave, single-mode quantum-cascade lasers at lambda similar or equal to 5.4 μm', *Appl. Phys. Lett.*, 2005, **86**, p. 041109
5 Bahriz, M., *et al.*: 'Room-temperature operation of $\lambda \approx 7.5$ μm surface-plasmon quantum cascade lasers', *Appl. Phys. Lett.*, 2006, **88**, p. 181103
6 Tredicucci, A., *et al.*: 'Single-mode surface-plasmon laser', *Appl. Phys. Lett.*, 2000, **76**, p. 2165
7 Carras, M., *et al.*: 'Photonic modes metallodielectric periodic waveguides in the midinfrared spectral range', *Phys. Rev. B*, 2006, **74**, p. 235120